Journal of Molecular Structure 1197 (2019) 645–655

Contents lists available at ScienceDirect

Journal of Molecular Structure

journal homepage: http://www.elsevier.com/locate/molstruc

Novel Cu(II), Co(II) and Zn(II) metal complexes with mixed-ligand: Synthesis, crystal structure, α-glucosidase inhibition, DFT calculations, and molecular docking

Davut Avcı [a, *], Sümeyye Altürk [a], Fatih Sönmez [b], Ömer Tamer [a], Adil Başoğlu [a], Yusuf Atalay [a], Belma Zengin Kurt [c], Necmi Dege [d]

[a] Sakarya University, Faculty of Arts and Sciences, Department of Physics, 54187, Sakarya, Turkey
[b] Sakarya University of Applied Sciences, Pamukova Vocational School, 54055, Sakarya, Turkey
[c] Bezmialem Vakif University, Faculty of Pharmacy, Department of Pharmaceutical Chemistry, 34093, Istanbul, Turkey
[d] Ondokuz Mayıs University, Faculty of Arts and Sciences, Department of Physics, 55139, Samsun, Turkey

ARTICLE INFO

Article history:
Received 12 May 2019
Received in revised form
1 July 2019
Accepted 8 July 2019
Available online 11 July 2019

Keywords:
2,2′-dipyridylamine
6−Methylpyridine−2−carboxylic acid
Metal ions
XRD
FT−IR and UV−Vis
α-Glucosidase
Docking
DFT//HSEh1PBE

ABSTRACT

Novel Cu(II), Co(II) and Zn(II) metal complexes containing 6−methylpyridine−2−carboxylic acid and 2,2′-dipyridylamine {[Cu(6-mpa)(dipya)(OAc)]·3H_2O (**1**), [Co(6-mpa)(dipya)Cl_2]·2H_2O (**2**), [Zn(6-mpa)$_2$(dipya)] (**3**)} were synthesized for the first time. Their structural and spectroscopic analyses were performed by XRD, LC-MS/MS, FT-IR and UV−Vis spectroscopic techniques. The DFT/HSEh1PBE/6−311G(d,p)/LanL2DZ level was also used to obtain optimal molecular geometry, vibrational wavenumbers, electronic spectral behaviors and major contributions to the electronic transitions for the complexes **1**−**3**. Their effects on α-glucosidase activity were evaluated. All complexes inhibited α-glucosidase with the IC_{50} values ranging from 513.10 to >600 μM. Finally, in order to display interactions between the synthesized complexes (**1**−**3**) and target protein (the template structure *S. cerevisiae* isomaltase), the molecular docking study was fulfilled.

1. Introduction

Due to their many potential applications such as catalysis, nonlinear optics, luminescence and ion exchange, the synthesis and physicochemical properties of pyridine derivatives, such as methylpicolinic acid, have been received great attention [1–5]. Furthermore, the ligands bearing conjugated electron-rich heteroaromatic rings, such as 2,2′-dipyridylamine, 1,10-phenanthroline, etc. are important in the understanding of electron transfer processes, mixed valence complexes and photochemistry. They are also used for the formation of different metal complexes including transition metals in biological processes [6–8]. Diabetes mellitus (DM) is a common degenerative disease and characterized by high blood glucose levels. Since the effective antidiabetic treatments attempt to decreasing blood glucose levels, keeping glucose under control is very important [9,10]. Considering the most common type 2 diabetes (T2DM) depending on insulin resistance, the prevalence of T2DM in all age groups is increasing in the world and it is estimated that it will reach 4.4% in the next ten years [11]. It is well-known that α-glucosidase inhibitors (AGIs) delay the digestion of carbohydrates and prolong the digestion time in general carbohydrates, as well as slow the absorption of glucose and thus blunt the increase of postprandial plasma glucose. AGIs reducing postprandial hyperglycemia remarkably play an important role in the treatment of T2DM and pre-diabetes situations. The positive effects of α-glucosidase inhibitors on both postprandial hyperglycemia and the reducing risk of developing type 2 diabetes in patients with impaired glucose resistance have been reported [12–14]. In spite of the variety of the available drugs, the response and efficacy of the therapy is overly-dependent on the patients. In this regard, the searching and development of novel and broad-spectrum antidiabetic agents have been encouraged several

* Corresponding author.
E-mail address: davci@sakarya.edu.tr (D. Avcı).

https://doi.org/10.1016/j.molstruc.2019.07.039
0022-2860/

research groups all around the world. In order to fulfill this goal, many natural and synthetic heterocyclic compounds (benzothiazole, oxadiazole, xanthones, flavonoid, pyrrolidine, indole analogues, etc.) have been investigated over the years, some of them showed inhibitor activity against a-glucosidase, which is one of the main targets of diabetes treatment [12,14–18]. However, the design and synthesis of high affinity glucosidase inhibitors are still great importance. In this direction, the healing effects of complexes containing different metal ions on individuals with Type 2 diabetes have been subject of intensive research. Particularly, metal complexes of nitrogen-containing ligands are frequently used in the field of coordination chemistry due to structurally, spectroscopically and catalytically similarity with some enzyme-substrate complexes in our body [19–25].

The inhibitor activity of various metal ions, such as Cu^{2+}, Zn^{2+}, V^{4+}, Ni^{2+}, Fe^{2+}, Mn^{2+}, etc., have been investigated against α-glucosidase [26]. Up till now, the different studies on the complex containing metal ions [27–30] have been reported. Besides, the insulinomimetic activity of different metal complexes including picolinic acid and its derivatives ($VO(pa)_2$ [31], $VO(6mpa)_2$, $VO(3\text{-}mpa)_2$ [32], $Cr(pa)_3$, $Mn(pa)_2$, $Mn(pa)_3$, $Fe(pa)_2$, $Fe(pa)_3$, $Co(pa)_2$, $Ni(pa)_2$, $Cu(pa)_2$ [33] and $Zn(pa)_2$, $Zn(3\text{-}mpa)_2$, $Zn(6\text{-}mpa)_2$ [34]) for the release of free fatty acid (FFA) from rat adipocytes have been examined. Lastly, the various metal complexes including picolinate (pa) and 6-methyl-2-picolinmethylamide (6mpa-ma) as α-glucosidase inhibitors have been obtained as $Cu(pa)_2$, $Zn(pa)_2$, $VO(pa)_2$ [35] and $Zn(6mpa–ma)_2SO_4$ [36]. To date, there are no α-glucosidase inhibition activity studies of the mixed ligand metal complexes including 6-mpa except for metal complexes of 6-mpa with thiocyanate and 4(5)-methlyimidazole in the literature [37,38].

The aim of our work is to synthesize novel mixed ligand metal complexes containing 6-methylpyridine-2-carboxylic acid (6-mpaH) and 2,2′-dipyridylamine (dipya) as effective α-glucosidase inhibitors. In this context, as a result of our ongoing works, novel Cu(II), Co(II) and Zn(II) complexes (complexes 1–3) containing 6-methylpyridine-2-carboxylic acid (6-mpaH) and 2,2′-dipyridylamine (dipya) were synthesized for the first time. The crystal structure of Cu(II) complex was determined by XRD spectroscopic technique, while molecular structures of Co(II) and Zn(II) complexes were defined by mass spectrometry (MS). The structure of complex **3** was also verified by the ^1H and ^{13}C NMR spectra. The α-glucosidase enzyme inhibition and electronic spectral behavior studies were experimentally surveyed. Furthermore, the structural, spectral, electronic, microscopic second- and third-order nonlinear optical parameters of complexes 1–3 in gas phase and ethanol solvent were examined by using DFT/HSEH1PBE/6-311G(d,p)/LanL2DZ level. After all, to determine the ligand protein interactions, molecular docking study was carried out.

2. Experimental and computational details

2.1. Physical measurements

FT-IR spectra of the novel synthesized complexes were recorded by using a PerkinElmer Spectrum-Two FT-IR spectrophotometer equipped with PerkinElmer UATR-TWO diamond ATR. The UV–Vis electronic absorption spectra of the complexes 1–3 were examined in the range of 900–200 nm by using a HITACHI U-2900 UV/VIS spectrophotometer in ethanol solvent with quartz cell of 1 cm. Mass spectra of the complexes 2,3 were obtained with SHIMADZU-8030 or AGILENT-6460 LC–MS/MS quadrupole mass spectrometer, equipped with an electrospray ionization (ESI +/−) used in MS/MS mode. The ^1H and ^{13}C NMR analysis of the complex **3** were acquired by a Varian Infinity Plus spectrometer at 300, 75 MHz, respectively.

2.2. X-ray structure determination

To collect data of suitable single crystal of the complex **1**, a Stoe IPDS II diffractometer using Mo–Kα (λ = 0.71073 Å) radiation at 296 K was used. The crystal structure determination details are given in Table 1. The crystal structure of the complex **1** was solved by direct methods using SHELXT [39] and refined by full-matrix least-squares methods on F^2 using SHELXL-97 [39]. The hydrogen atoms bonding to carbon atoms were located from different maps and then treated as riding atoms with C–H distances of 0.96 Å. The H atoms of water were located in a different map refined freely. Molecular diagrams were created using MERCURY [40]. Supramolecular analyses were made and the diagrams were prepared with the aid of PLATON [41].

2.3. Materials and synthesis of the complexes 1–3 {[Cu(6-mpa)(dipya)(OAc)]·3H$_2$O, (**1**), [Co(6-mpa)(dipya)Cl$_2$]·2H$_2$O, (**2**), [Zn(6-mpa)$_2$(dipya)], (**3**)}

All of the chemical reagents used in this study were analytical grade commercial products. 6-mpaH (6-Methylpyridine-2-carboxylic acid), 2,2′-Dipyridylamine (dipya), copper(II) acetate hydrate ($Cu(OAc)_2\cdot H_2O$), cobalt(II) chloride hexahydrate ($CoCl_2\cdot 6H_2O$) and zinc(II) acetate dihydrate ($Zn(OAc)_2\cdot 2H_2O$) were purchased from Sigma-Aldrich. The synthesis methods of the complexes **1**–**3** are as follows (see Scheme 1):

Synthesis of the complex **1:** An aqueous solution (10 mL) of 2,2′-dipyridylamine (1 mmol) was slowly added to a solution of metal salt (1 mmol) dissolved in water (5 mL). After being stirred for 45 min, the mixture was added to a solution of 6-methylpyridine-2-carboxylic acid (1 mmol) dissolved in ethanol (5 mL). The last mixture was stirred at 60 °C for 4 h, and evaporated for a month at room temperature [42]. At the end of this process, the formed crystals for complex **1** were filtered off, washed thoroughly with distilled water, and finally air-dried at room temperature. The single crystals for the complex **1** were obtained as blue in prism shaped.

Synthesis of the complex **2**: The solid 6-methylpyridine-2-carboxylic acid (1 mmol), 2,2′-dipyridylamine (1 mmol) and

Table 1
Crystal data and structure refinement parameters for the complex **1**.

Empirical formula	$C_{19}H_{18}CuN_4O_4\cdot 3(H_2O)$
Formula weight	483.96
Crystal system	Triclinic
Space group	P–1
Temperature	296
Radiation type	Mo *Kα*
Wavelength	0.71073
Crystal size (mm)	0.78 × 0.61 × 0.38
a (Å)	7.829 (8)
b (Å)	9.776 (10)
c (Å)	14.874 (14)
α (°)	96.432 (8)
β (°)	104.575 (7)
γ (°)	103.068 (8)
V (Å^3)	1055.77 (19)
Z	2
F(000)	502
Density (g cm^{-3})	1.522
μ (mm^{-1})	1.08
θ range (°)	1.4–27.5
Measured refls.	14175
Independent refls.	4147
R_{int}	0.075
S	1.11
R1/w*R*2	0.047/0.124
max/min (eÅ^{-3})	0.71/−0.64

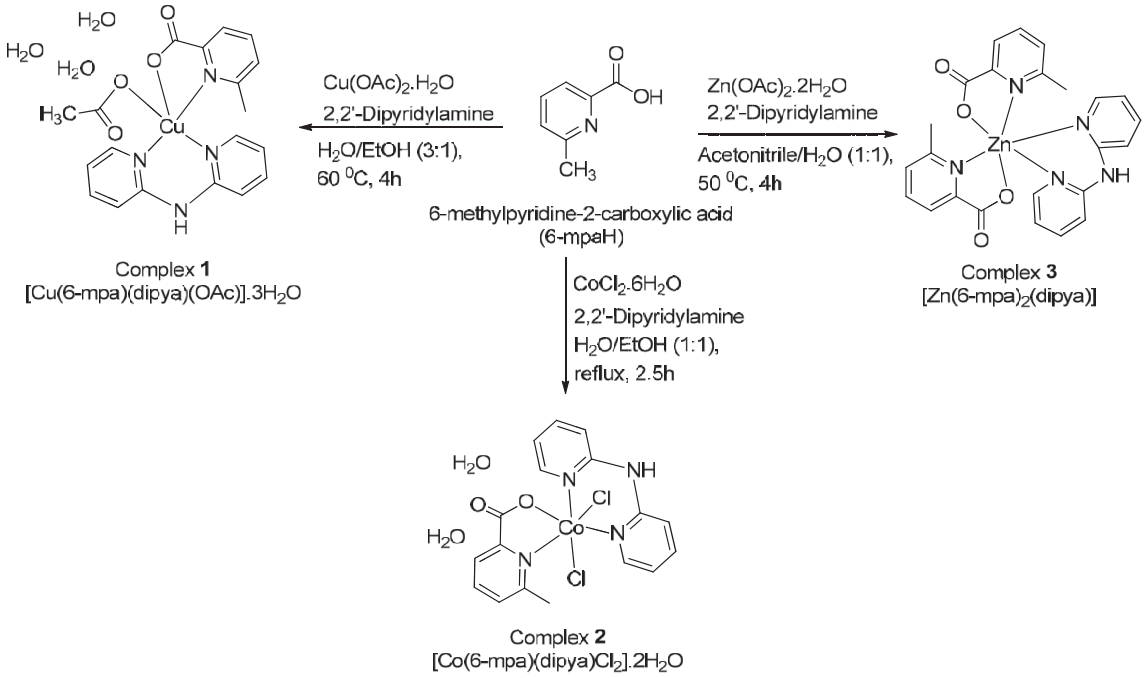

Scheme 1. The synthesis of the complexes **1**–**3**.

cobalt(II) chloride hexahydrate (1 mmol) were added to a mixture of ethanol and water (20 mL, 1:1) under continuous stirring at 70 °C. This mixture was refluxed for 4 h and allowed to evaporate at room temperature [42]. After the period of 18 days, the powder product for the complex **2** was filtered off, washed thoroughly with distilled water, and finally air-dried at room temperature. Anal. Calc. for $C_{17}H_{19}Cl_2N_4O_4Co$ (complex **2**): C, 43.15; H, 4.05; N, 11.84. Exact mass (*m*/*z*): 472.01. Found: ESI-LC-MS/MS (*m*/*z*): 471 ($[M]^+$). The mass spectrum for the complex **2** is given in Fig. S1.

Synthesis of the complex **3**: The solid 6-methylpyridine-2-carboxylic acid (2 mmol), 2,2′-bipyridyl (2 mmol) and zinc(II) acetate dihydrate (1 mmol) were added to a mixture of acetonitrile and water (20 mL, 1:1) under continuous stirring at 50 °C. The last mixture was stirred within closed vial at 50 °C for 2.5 h and evaporated for 15 days at room temperature [43]. At the end of this process, the powder product for the complex **3** was filtered off, washed thoroughly with distilled water, and finally air-dried at room temperature. Anal. Calc. for $C_{24}H_{21}N_5O_4Zn$ (complex **3**): C, 56.65; H, 4.16; N, 13.76. Exact mass (*m*/*z*): 507.09. Found: ESI-LC-MS/MS (*m*/*z*): 507.3 ($[M]^+$). ^{1}H NMR (DMSO-d_6, 300 MHz) δ/ppm: 2.72 (6H, s), 6.82–6.86 (2H, td, $J_1 = 1.2$ Hz, $J_2 = 3.9$ Hz), 7.60–7.71 (5H, m), 8.01–8.09 (5H, m), 8.18–8.20 (2H, dt, $J_1 = 0.9$ Hz, $J_2 = 4.1$ Hz), 9.63 (NH, br); ^{13}C NMR (DMSO-d_6, 75 MHz) δ/ppm: 25.4, 114.3, 118.4, 123.6, 130.1, 140.1, 143.2, 149.9, 152.3, 157.0, 159.6, 168.3. The mass spectrum, ^{1}H and ^{13}C NMR spectra of the complex **3** are given in Figs. S2 and S3.

2.4. α-Glucosidase inhibition assay

α–Glucosidase inhibition activities of the synthesized complexes **1**–**3** were investigated by doing small changes on Sun's protocol [44]. The α–glucosidase from Saccharomyces cerevisiae (Sigma, G5003) was determined as the target protein using p–nitrophenyl–α–D–glucopyranoside (pNGP, Sigma, N1377) as the substrate. The compounds and genistein were dissolved in DMSO. The enzyme and the substrate were dissolved in potassium phosphate buffer (0.05 M, pH 6.8). The enzymatic reaction mixture composed of α-glucosidase (0.02 U, 20 μL), substrate (1.25 mM, 30 μL), test compounds (10 μL) and potassium phosphate buffer (140 μL) was incubated at 37 °C for 30 min. After 30 min of incubation, the absorbance of yellow color produced due to the formation of p-nitrophenol was measured using Synergy H1 (BioTek, USA) 96-well microplate reader at 405 nm. All experiments were performed in triplicates. The surveying of α–glucosidase inhibition activity for the complexes **1**–**3** was fulfilled on the basis of our previously reported study [37,38],

$$\textit{Glucosidase inhibition} = [(A_c - A_s)/A_c] \times 100$$

where A_c is the absorbance of control and A_s is the absorbance of samples, respectively. The calculation of IC_{50} values was performed by using Graphpad Software.

2.5. Computational procedure

To survey quantum chemical calculations of the synthesized complexes **1**–**3**, GAUSSIAN 09, Revision D01 [45], and GaussView 5 program [46] were used. The DFT/HSEh1PBE hybrid density functional [47,48] and the combined basis set of 6-311G(d,p) [49] for C, N, O, H atoms, and LanL2DZ [50] for Cu, Co and Zn atoms were selected to obtain the reasonable results for the ground state geometries and vibrational wavenumbers of the complexes **1**–**3**. To examine the electronic spectral parameters of complexes **1**–**3** in ethanol solvent and gas phase, the time dependent DFT/HSEh1PBE (TD–DFT/HSEh1PBE) level [51] with conductor–like polarizable continuum model (CPCM) [52] was applied. Frontier molecular orbital (FMO) energies and some related parameters were investigated at the same level. Natural bond orbital (NBO) analysis [53]

was performed to define coordination environment around the metal ion centers and hydrogen bonding interaction. The microscopic linear optical (LO) polarizability (α and Δα), second- and third-order nonlinear optical (NLO) parameters (β and γ) of the complexes **1**–**3** in gas phase and ethanol solvent were obtained at the same level. Additionally, the molecular electrostatic potential (MEP) surfaces of the complexes **1**–**3** were examined by using the same method.

2.6. Docking procedure

In order to investigate protein-ligand interactions between the synthesized complexes (**1**–**3**) and target protein (the template structure *S. cerevisiae* isomaltase (PDBID: 3A4A)) used as rigid, we performed the molecular docking study by using the iGEMDOCK program [54]. The ligand structures were selected as the ground state energy conformations of each synthesized complexes obtained by GAUSSIAN program. GEMDOCK parameters in the flexible docking were applied as the initial step sizes ($\sigma = 0.8$ and $\psi = 0.2$; step-size vectors of decreasing-based Gaussian mutation and self-adaptive Cauchy mutation, respectively), family competition length ($L = 2$), population size ($N = 800$), and recombination probability ($p_c = 0.3$). For each ligand screened, when the convergence falls below a certain threshold or reaches a maximum preset value of 80, GEMDOCK was set to stop optimization. Thus, GEMDOCK provided 800 solutions in one generation and terminated after it finished 64 000 solutions for each docked ligand.

3. Results and discussion

3.1. Molecular geometries of the synthesized complexes *1*–*3*

The synthesis procedures for complexes **1**–**3** are given in Scheme 1. The single crystal structure of complex **1** was determined by X-ray diffraction analysis. Table 1 depicts the crystal data and structure refinement parameters of complex **1**. The complex **1** crystallizes in the triclinic space group P-1. Fig. 1 shows the crystal and optimized theoretical molecular structures of the complexes **1**–**3**. The coordination around Co(II) and Zn(II) atoms in complexes **2,3** are similarly described as a distorted octahedron geometry while the coordination around Cu(II) atom in complex **1** is determined as a distorted trigonal bipyramidal geometry. The complex **1** contains a central Cu(II) ion coordinated by 6-mpa, dipya and acetate ligands. The complex **2** consists of Co(II) central ion coordinated by 6-mpa and dipya ligands, and two chlorine atoms, while the complex **3** includes a Zn(II) ion coordinated by two 6-mpa and dipya ligands.

As can be seen in Fig. 1, N, O atoms of pyridine and carboxylate parts constitute the five membered chelate rings formed by coordinating to Cu(II), Co(II) and Zn(II) centers. Similarly, six membered rings consist of the centers of Cu(II), Co(II) and Zn(II) with pairs of *cis* nitrogen donor atoms belonging to chelating 2,2′-dipyridylamine ligands. The M(II)–N1 and M(II)–O2 bond lengths for complex **1** have been observed at the range of 2.019(3) and 2.154(2). These distances for the complexes **1**–**3** have been calculated at the range of 1.991–2.176 and 1.875–2.174 Å by HSEh1PBE level. These results are consistent with the same bond lengths in previously reported metal complexes containing picolinate ligand [37,55–58] (see Table S1). Considering the coordination of M(II) centre with N atoms of dipya, the Cu/Co/Zn–N bond distances changed with coordination around M(II). The O–M–N and N–M–N bond angles belonging to five/six-membered chelate ring formed by metal(II) ion and coordinated O and N atoms of 6-mpa ligand/N atoms of dipya ligand are obtained at the range of 78.0–83.2° and 76.4–91.5° by HSEh1PBE level, respectively (see Table S1). These angles for complex **1** were observed at 80.0(11) and 89.5(11)°, respectively. The bond lengths and angles belonging to the coordination geometry around Cu(II), Co(II) and Zn(II) atom for complexes **1**–**3** are consistent with previously reported values of different complex structures [37,59].

The crystal packing structure of complex **1** displays the O–H···O type intermolecular hydrogen bonding interactions among the carboxylate group of 6-mpa ligand, oxygen atom of acetate ligand and three water molecules (see Fig. 2). The D···A bond lengths showing O–H···O type intermolecular hydrogen bonding interactions were observed range from 2.833(4) to 2.923(4) Å. All possible interactions together with symmetry codes for the complex **1** are presented in Table 2.

3.2. Vibrational frequencies

We have investigated the FT–IR spectra and theoretical vibrational frequencies for the complexes **1**–**3** in order to assign vibrational modes and determine coordination environment around the M(II) for complexes **1**–**3**. Table 3 depicts theoretical results obtained by HSEh1PBE/6-311G(d,p)/LanL2DZ level and scaled by 0.96 [60]. Fig. 3 represents the FT–IR spectra of the complexes **1**–**3**. It was reported that the stretching vibrations of OH and NH group approximately appear at the range of 3700–3500 and 3500–3300 cm^{-1} [61]. The OH stretching vibration modes of uncoordinated water molecules in complexes **1,2** were observed range from 3248 to 3507 cm^{-1}, the corresponding modes were

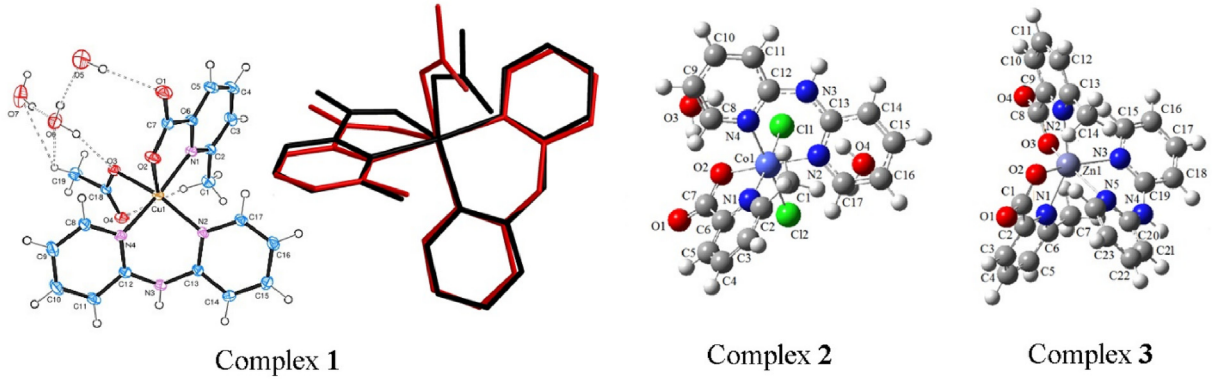

Fig. 1. The single crystal structure and superimposed structure of theoretical (red stick) and experimental (black stick) structures for the complex **1** except for hydrogen atoms, and the optimized molecular structures of the complexes **2** and **3** at HSEh1PBE/6–311G(d,p)/LanL2DZ.

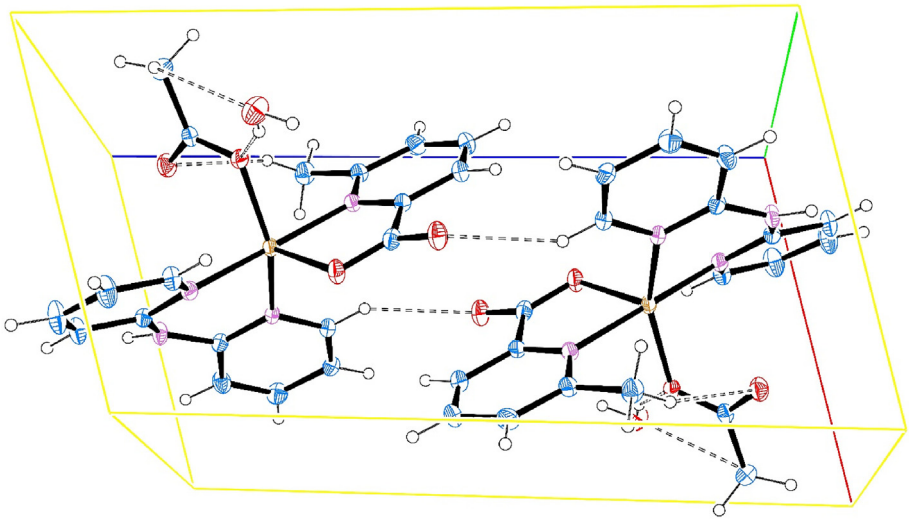

Fig. 2. The crystal packing structure of the complex **1**.

Table 2
Hydrogen–bond parameters for the complex **1** (Å and °).

D–H· · ·A	D–H	H···A	D···A	D–H···A
O6–H6A· · ·O3	0.82 (2)	2.06 (2)	2.861 (4)	167 (4)
O6–H6B· · ·O5	0.79 (2)	2.05 (2)	2.833 (4)	171 (5)
O5–H5A· · ·O1	0.81 (2)	2.14 (2)	2.923 (4)	163 (5)
O7–H7A· · ·O6	0.84 (2)	2.06 (2)	2.866 (5)	161 (4)
N3–H3· · ·O4^{i}	0.86	1.96	2.777 (4)	159
O5–H5B· · ·O1^{ii}	0.81 (2)	2.28 (4)	2.961 (4)	142 (5)
O7–H7B· · ·O2^{iii}	0.83 (2)	2.07 (2)	2.875 (4)	165 (4)

Symmetry codes: (i) –x+1, –y+1, –z+2; (ii) –x+1, –y+2, –z+1; (iii) x–1, y, z.

calculated at 3456–3780 cm^{-1} range (see Table 3). The NH stretching vibration modes belonging to the dipya ligand for complexes **1**–**3** were observed at 3423, 3217, 3354 cm^{-1}, the corresponding modes were calculated at 3518, 3526, 3512 cm^{-1}, respectively. This NH broad band was confirmed by previously reported studies [43,62]. This peak is observed as a broad band due to high electron delocolization in the dipya ligand and electron transitions arisen from coordination. It is well known that the CH stretching vibrations of the aromatic and aliphatic molecules emerge at above 3000 and below 3000 cm^{-1}, respectively [61]. The ring CH stretching vibration modes of 6-mpa and dipya ligands appeared at above 3000 cm^{-1}, as can be shown in FT–IR of the complexes **1**–**3** (see Table 3). The CN stretching vibrational modes of 6-mpa ligand for the complexes **1**–**3** emerged at 1533, 1557, 1274 cm^{-1}, respectively, these modes were found to be 1575, 1573, 1276 cm^{-1} by HSEh1PBE/6-311G(d,p)/LanL2DZ level. These results exhibit that there is a good agreement between experimental and theoretical vibrational wavenumbers. The CH in-plane bending vibrational peaks of 6-mpa ligand arisen approximately at 1400 cm^{-1} are consistent with previously reported results [37,63].

As can be seen in Fig. 3, the asymmetric/symmetric COO^{-} stretching modes from FT-IR spectra of complexes **1**–**3** were found to be 1651/1372, 1651/1305 and 1637/1314 cm^{-1}. These differences between experimental/theoretical asymmetric/symmetric COO^{-} modes found at 346–279/435–355 cm^{-1} range display that 6-mpa ligand coordinates to metal ions as a monodentate ligand via carboxylate group. These results are coherent with different metal complexes [37,55–58,63,64]. Besides, the experimental/theoretical peaks arising from COO^{-} stretching mode of OAc ligand for the complex **1** were found to be 1585/1645 cm^{-1} (see Table 3). The other detailed vibrational modes belonging 6-mpa, dipya, acetate and water ligands were assigned in Table 3.

Table 3
Comparison of the FT–IR and calculated vibration frequencies for the complexes **1**–**3.**

Assignments	Complex **1**		Complex **2**		Complex **3**	
	FT–IR	HSEh1PBE	FT–IR	HSEh1PBE	FT–IR	HSEh1PBE
ν OH	3507	3780	3351	3719	–	–
ν NH	3423	3518	3217	3526	3354	3512
ν OH	3309	3456	3248	3636	–	–
ν CH dipya	3140	3115	3140	3160	3178	3135
ν CH 6-mpa		3113	3109	3108	3089	3110
ν CH dipya	3084	3109	3083	3105	3069	3107
ν CH_3 OAc	2991	3047	–	–	–	–
ν CH_3 6-mpa	2911	3022	2988	3043	3017	3028
ν COO^{-} 6-mpa	1651	1693	1651	1748	1637	1721
β HOH		1651	1597	1628	–	–
ν COO^{-} OAc	1585	1645	–	–	–	–
ν NC dipya	1563	1624		1595	1590	1591
ν CC 6-mpa		1602		1622	1618	1601
ν CC dipya	1564	1591		1610	1531	1610
β HCC dipya		1582	1481	1484	1480	1479
ν NC 6-mpa	1531	1575	1557	1573	1274	1276
β HCC 6-mpa		1575	1451	1450		1448
β HCH 6-mpa	1476	1452	1417	1437	1464	1451
β HCH OAc	1411	1423	–	–	–	–
ν COO^{-} OAc	1404	1368	–	–	–	–
ν COO^{-} 6-mpa	1372	1338	1305	1313	1314	1337
γ HCCC dipya	1011	1020	939	969	962	971
γ HCCC 6-mpa	907	989	983	988	989	986
γ HOHO	770	769	527	567	–	–
γ CZnCN	–	–	–	–	712	711
γ CCNCu	538	499	–	–	–	–
ν CoO	–	–	507	465	–	–
γ ZnCCN	–	–	–	–	433	439
β CoNC	–	–	408	402	–	–
ν CoCl	–	–		348	–	–

υ: Stretching; β: in plane bending; γ: out-of plane bending.

3.3. The electronic absorption spectra, FMOs, MEP and NBO parameters

The TD–HSEh1PBE-6–311G(d,p)/LanL2DZ level was used to interpret the electronic absorption spectra, major electronic transitions and oscillator strengths. Fig. 4 depicts the UV–Vis spectra of

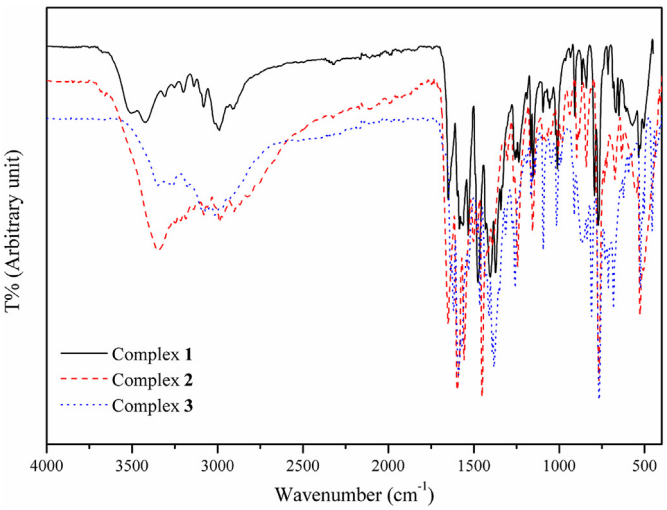

Fig. 3. The FT–IR spectra of the complexes **1**–**3**.

the complexes **1**–**3** in ethanol solvent. The remarkable contributions from FMOs to the electronic transitions were described by using SWizard [65] program. The electronic spectral parameters are comparatively given in Table S2. Theoretical absorption peaks for complexes **1,2** corresponding the highest electronic absorption wavelength in ethanol solvent were appointed as d→d transition. This transition formed from metal to metal charge transfer (MMCT), from metal to ligand and from ligand to metal charge transfer (MLCT) transitions (see Table S2 and Fig. 5). These peaks for complexes **1,2** in ethanol solvent were calculated at 594 and 586 nm with the contributions H−13→L β(+15%)/H−17→L β(+13%) and H–9→L+1 (+10%)/H–17→L+1 (+9%), respectively. The absorption peaks of the complexes **1**–**3** in ethanol solvent arisen from n→π* and π→π* transitions exhibiting metal–ligand and ligand–ligand charge transfers emerged at the range of 384–219, 320–200 and 311–227 nm. The corresponding theoretical peaks in ethanol solvent were found to be 364–244, 320–235 and 299–227 nm range. It is clear that the remarkable contributions to electronic transitions originated from different frontier molecular orbitals, as can be seen in Table S2. It is concluded from Fig. 5 that the low absorption bands of complexes **1**–**3** arisen from intraligand charge transfer (ILCT).

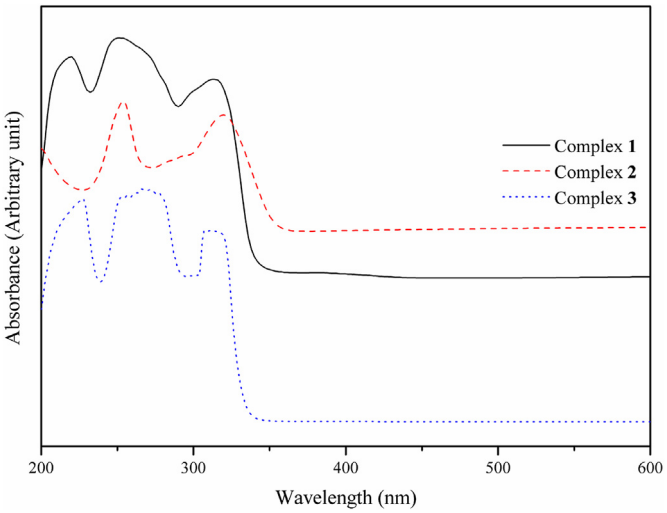

Fig. 4. The UV–Vis spectra in ethanol solvent of the complexes **1**–**3.**

Considering the Tauc and Menth's equation [56,66], the optical band gap energy values are calculated by using following equation

$$(\alpha h\nu) = C\left(h\nu - E_g\right)^{1/2} \quad (1)$$

where the absorption coefficient α is obtained by $\alpha = 2.303A/d$ formula (A is the absorbance in the UV–Vis region and d is the cuvette length (1 cm)), C is a proportionality constant related to the effective masses associated with the bands, $h\nu$ is the photon energy and E_g is the direct band gap energy. According to Fig. 6, the E_g band gap energy values of the complexes **1**–**3** were found to be 4.70, 4.92 and 5.15 eV, respectively (see Fig. 6). The theoretical energy gap obtained from FMO energies were calculated at 4.40 for α spin, 3.34 and 4.32 eV.

In this context, to determine the relationship among the physicochemical properties of the molecules, such as molecular chemical stability and chemical reactivity, we examined energy gap results. To obtain FMO energy values of the complexes **1**–**3** in ethanol solvent, the HSEH1PBE/6-311G(d,p)/LanL2DZ level was used. It could be usually noted that the electron donating and electron withdrawing ability symbolize the HOMO and LUMO, respectively. The FMO energy values of the complexes **1**–**3** in ethanol solvent were obtained at −6.44 for α spin, −6.51, −6.25 eV (HOMO), −2.05 for α spin, −3.17, −1.93 eV (LUMO), as can be seen in Fig. 5. The χ, η and S parameters, called as electronegativity, chemical hardness and softness, obtained from FMO energies are computed by using equations given references therein [56,67]. The χ parameters for the complexes **1**–**3** were found at 4.25 for α spin, 4.54 for β spin (complex **1**), 4.84 (complex **2**), 4.09 (complex **3**) eV. The η and S parameters for the complexes **1**–**3** were calculated at 2.20 for α spin, 1.90 for β spin (complex **1**), 1.67 (complex **2**), 2.16 (complex **3**) eV, and 0.46 for α spin, 0.53 for β spin (complex **1**), 0.60 (complex **2**), 0.46 (complex **3**) eV^{-1}, respectively. It could be concluded from these results that the complex **2** with smaller η parameter, higher χ and S parameters provided the more efficient charge transfer, and could be easily polarized. The main reason is due to the effect of d-orbital occupation on the coordination geometry of the complexes.

The NBO calculations for the complexes **1**–**3** were obtained by using HSEh1PBE/6-311G(d,p)/LanL2DZ level. To survey inter- and intra-molecular bonding, and interactions among bonds in coordination environments of M(II) ions, as well as charge transfer or conjugative interaction in molecular system, NBO study was performed. In this NBO analysis, the intense interaction between electron donors and acceptors, and the degree of conjugation of the investigated molecular system were evaluated by determining the higher stabilization energies ($E^{(2)}$). The second-order perturbation approach [56,68,69] was applied to investigate the hyperconjugative interaction energies. The delocalization between lone-pair (n) orbitals of nitrogen/oxygen/chloride atom and anti-lone-pair (n*) orbitals of M(II) ion was clearly determined (see Table S3). This delocalization effect playing significant role on the coordination environments of the Cu(II), Co(II) and Zn(II) ions in the complexes **1**–**3** was appointed as n→n* interactions. The coordination environments of M(II) ions were verified by these interactions obtained at the range from 15.69 to 66.82 kcal/mol for the complexes **1**–**3**. The $E^{(2)}$ values for the complexes **1**–**3** defined as the stabilization energy were found range from 74.04 to 0.51 kcal/mol. Moreover, the stabilization interactions as well as hydrogen-bonding interactions for the complex **1** among the carboxylate group of 6-mpa ligand, oxygen atom of acetate ligand and three water molecules were given in Table S3. The $E^{(2)}$ values of hydrogen-bonding interactions for the complex **1** were found at the range of 1.23 and 9.35 kcal/mol.

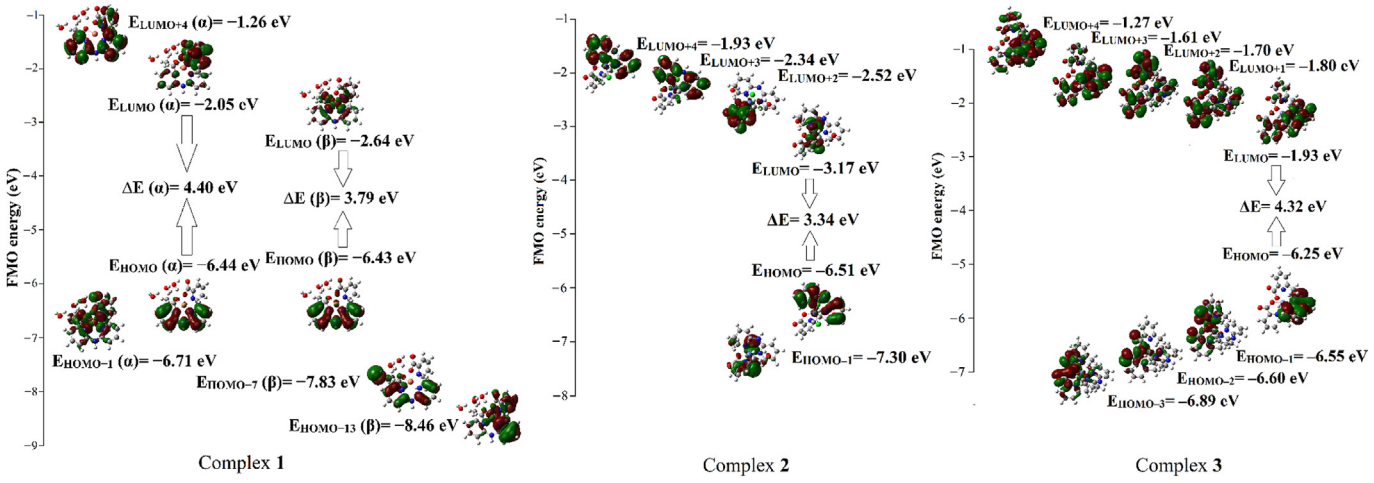

Fig. 5. The most active occupied and unoccupied molecular orbitals in electronic transition of the complexes **1**–**3** obtained by HSEh1PBE level in ethanol solvent.

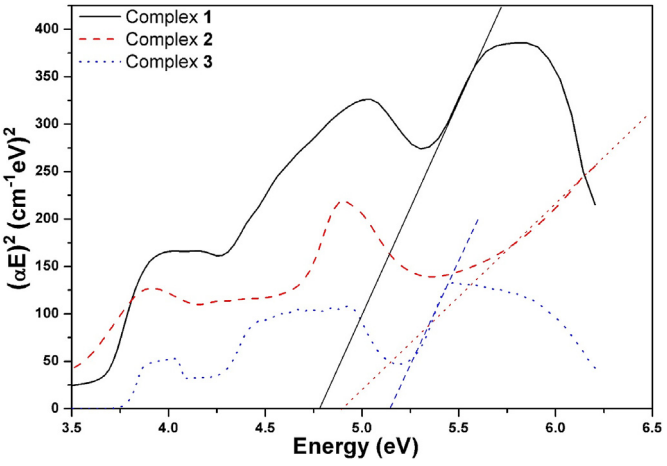

Fig. 6. The graphs of optical band gap energy for the complexes **1**–**3**.

The MEP surface is remarkably used in the research of relation between structure-activity and physicochemical properties of compounds containing biomolecules and drugs [70,71]. The MEP describes molecular shape, size and ESP regions interconnecting color classification at the same time. Fig. 7 displays the MEP surfaces of complexes **1**–**3**. The MEP color code values between the deepest red and blue for the complexes **1**–**3** are the range from −9.934e−2 to 9.934e−2 a.u., from −0.174e−2 to 0.174e−2 a.u. and from −9.397e−2 to 9.397e−2 a.u., respectively. The negative regions emerged at red color determining electrophilic reactivity are over the electronegative O atoms belonging the carboxylate groups and water ligands uncoordinated with M(II) ions. The positive regions appeared at blue color describing nucleophilic reactivity are over the H atom belonging to N atom of dipya ligand, as can be seen in Fig. 7.

3.4. The NLO parameters

Lately, due to engaging applications in the field of optical communication, optical switching and dynamic image processing, etc. [72–74], the development of device application for organic, inorganic and organometallic NLO materials is possible with involving both theoretical and experimental studies in different fields, such as physics, engineering, etc. Theoretical calculations provide an important contribution to understand the electronic polarization underlying the molecular NLO processes and establish of structure–property relationships.

The HSEH1PBE level was used to investigate the LO and NLO parameters of the complexes **1**–**3** in gas phase and ethanol solvent. By using equations given references therein [56,57,74], the α, Δα, β and γ parameters of the complexes **1**–**3** in gas phase and ethanol solvent were calculated (see Table S4). It could be noted that all LO

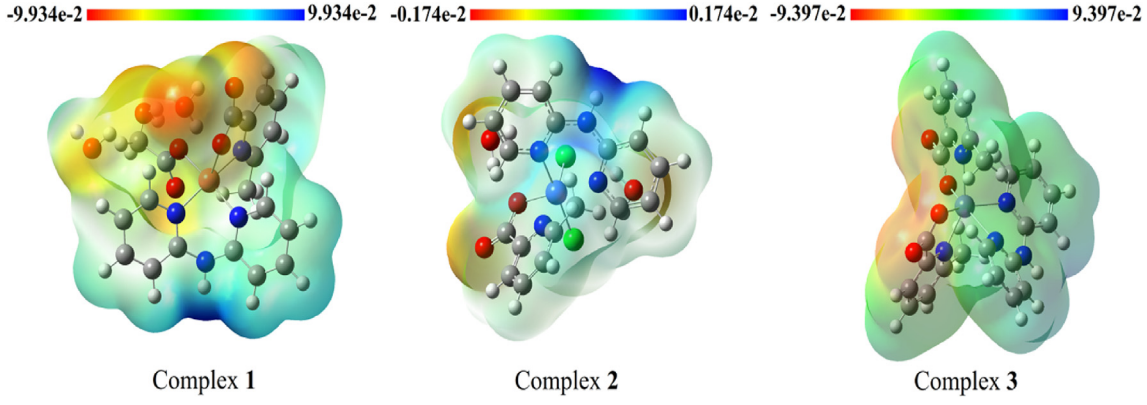

Fig. 7. Molecular electrostatic potential (MEP) surfaces for the complexes **1**–**3** obtained by HSEh1PBE level in gas phase.

and NLO parameters of the complexes **1**–**3** are observed with the substantial difference/similarity owing to M(II) ions and their coordination environments. Due to the d-orbital effect on the coordination geometry around M(II) ions, there is not observed remarkable difference between second-order β and third-order γ parameters for the complexes **1**–**3**. In comparison of LO and NLO parameters for molecular systems without experimental measurements, the results of p-Nitroaniline (pNA), nitrobenzene [75–77] and urea [78], which are the prototypical compounds, were used. The β values of the complexes **1**–**3** in gas phase/ethanol solvent were found to be $7.2 \times 10^{-30}/7.4 \times 10^{-30}$, $8.1 \times 10^{-30}/10.6 \times 10^{-30}$ and $5.0 \times 10^{-30}/3.0 \times 10^{-30}$ esu, respectively. From Table S4, the largest β value obtained for the complex **2** in gas phase and ethanol solvent are 8.1×10^{-30} and 10.6×10^{-30} esu. These results demonstrate that the β parameter for the complex **2** is 62.30/0.88 and 81.54/1.15 times higher than those of urea (0.130×10^{-30} esu)/pNA (9.2×10^{-30} esu). Unlike, the γ values for complex **2** in gas phase and ethanol solvent are found to be 26.8×10^{-36} esu and 77.2×10^{-36} esu, respectively. These values are about 1.79 and 5.15 times higher than that of pNA (15×10^{-36} esu). According to calculated β and γ parameters in gas phase and ethanol solvent, the complex **2** is a powerful indicator for microscopic second−order NLO property whereas the complexes **1,3** are remarkable indicator for microscopic third−order NLO property. The linear optical polarizability (α) values of the complexes **1**–**3** in mentioned solvents are calculated at $42 \times 10^{-24}/56.1 \times 10^{-24}$, $42.2 \times 10^{-24}/58.8 \times 10^{-24}$ and $46.1 \times 10^{-24}/62.4 \times 10^{-24}$ esu, respectively. It is clear that all of the calculated α values for the complexes **1**–**3** are higher than that of pNA (17×10^{-24} esu). According to our previous results, all results are comparable for the same parameters [37,38,56,57]. It could be interpreted that the main reasons for the change in the NLO parameters of these complexes are the different substitution and metal ions in coordination. In brief, it can be said that second−order NLO parameter for the complex **2** and third−order NLO parameters for the complexes **1,3** are notable.

3.5. α-Glucosidase inhibition studies

The α-glucosidase activity studies of the synthesized complexes (**1**–**3**) were fulfilled according to literature [37,41]. Table 4 demonstrates the IC_{50} values for α-glucosidase inhibitions of the complexes **1**–**3**. The IC_{50} values were obtained range from 513.10 μM to >600 μM. The complex **1** displayed the strongest inhibitor activity against α-glucosidase with the IC_{50} value of 513.10 μM. This value is 1.77-fold higher and 40.40 lower than those of acarbose ($IC_{50} = 906$ μM) [79,80] and resveratrol ($IC_{50} = 12.70$ μM) [81,82], well-known as α-glucosidase inhibitors, respectively.

The following points could be concluded from Table 4 with regard to structure-activity relationship (SAR):

(i) The complex **1** ($IC_{50} = 513.10$ μM) has a distorted trigonal bipyramidal geometry whereas the complexes **2** and **3** ($IC_{50} = >600$ μM) have a distorted octahedron geometry. This difference of coordination for complex **1** displays minor variation for enzyme activity.

(ii) Among complexes with the same coordination (complexes **2** and **3**), the changing metals and the coordination environment of Co(II) and Zn(II) ions have not showed a significant effect on α-glucosidase inhibition. According to the results of molecular docking, although complex **3** has more van der Waals interactions with the amino acid residues in the active site of the enzyme, its coordination environment and these interactions site did not significantly affect α-glucosidase inhibition.

Table 4
In vitro inhibition IC_{50} values (μM) of the complexes **1**–**3** for α−glucosidase.

Compound	IC_{50} (μM)[a]
6−Methylpicolinic acid (6-mpaH)	not active
2,2′−Dipiridilamin (dipya)	not active
Complex **1** [Cu(6-mpa)(dipya)(OAc)]·$3H_2O$	513.10 ± 0.75
Complex **2** [Co(6-mpa)(dipya)Cl_2]·$2H_2O$	>600
Complex **3** Zn(6-mpa)$_2$(dipya)	>600
Genistein	16.575 ± 0.23
Acarbose[b]	906
Resveratrol[c]	12.70

[a] IC_{50} values represent the means ± S.E.M. of three parallel measurements ($p < 0.05$).
[b] From ref. [79,80].
[c] From ref. [81,82].

So far, the IC_{50} values of various metal complexes of picolinate (pa) and 6-methyl-2-picolinmethylamide (6mpa-ma) for α-glucosidase inhibition have been reported at 1.28 μM, 15.4 μM, >1 mM, 9.6 μM for Cu(pa)$_2$, Zn(pa)$_2$, VO(pa)$_2$ [35] and Zn(6mpa-ma)$_2$$SO_4$ [36] complexes, respectively. Up to now, many organic molecules (oxadiazole, xanthones, flavonoid and indole analogues, etc.) have been synthesized as α-glucosidase inhibitors [12,15–18]. The inhibition values of them were observed at low micromolar. These compounds have stronger inhibitory activity than the synthesized complexes in this study. Moreover, α-glucosidase inhibition values of our previously synthesized mixed-ligand (6-mpa with NCS and MeI ligands) metal complexes were obtained at the range of 2.91 μM and >600 μM [37,38]. In present work, among the synthesized mixed-ligand (6-mpa and dipya) complexes of Cu(II), Co(II) and Zn(II) metals, the Cu(II) complex has the most effective inhibitory activity against α-glucosidase.

3.6. Molecular docking

So as to show protein-ligand interactions between the synthesized complexes (**1**–**3**) and target protein (the template structure *S. cerevisiae* isomaltase (PDBID: 3A4A)), we carried out the molecular docking study by using the iGEMDOCK program [54]. To investigate in vitro results, the results of electrostatic (E), hydrogen-bonding (H), and van der Waals (V) interactions for the protein-complex interaction profiles were determined. Table S5 depicts the estimated interactions and theirs energy values for the complexes **1**–**3**. The stabilized structures due to the interacting of complex structures with amino acid residues through some hydrogen-bonding and van der Waals interactions are given in Fig. 8. It is concluded that the variations of energy values of V interactions forming between the same amino acid residues and non-coordinated parts of ligands around Cu(II), Co(II) and Zn(II) ions depend on ligand and metal type.

Complex **1** (513.10 ± 0.75 μM), which is a Cu metal ion complex, exhibited the high inhibitor activity against α-glucosidase among complexes having dipya ligand substitution. According to docking results, total energy value of complex **1** calculated at −91.8 kcal/mol are higher than those of the complexes **2** and **3**. In the different amino acid residues interactions, the total hydrogen bonding interaction energy values for complexes **1**–**3** were found range from −3.5 to −6.7 kcal/mol. In general, the H bonding interactions for complexes **1**–**3** originate from the nitrogen atom of dipya ligand with OD, NZ of same or different amino acid residues. Although the H interactions for the complex **1** emerge higher than the complexes **2** and **3**, there are no major difference among the α-glucosidase enzyme inhibition results. For complex **1**–**3**, prominent H-interactions obtained at −3.2 and −3.5 kcal/mol energy values are

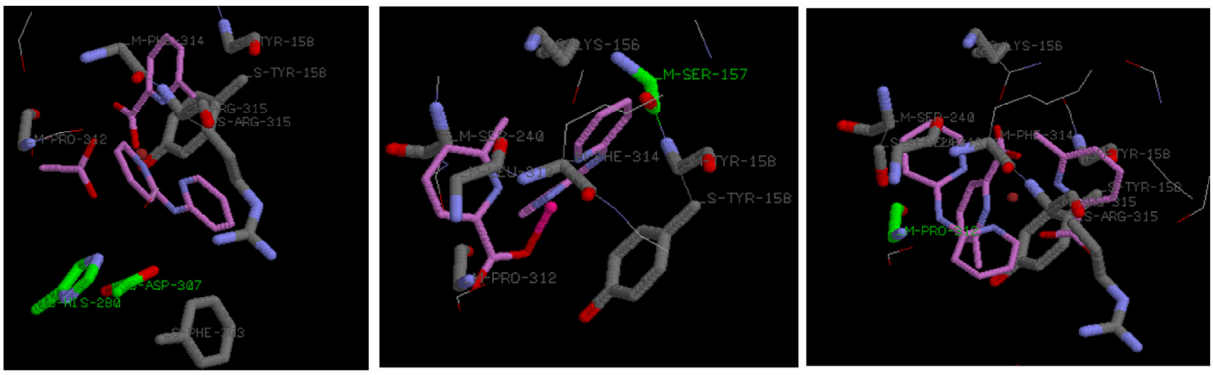

Complex **1** Complex **2** Complex **3**

Fig. 8. 3-D structures showing interactions between main/side chain amino acids and ligand of the complexes **1**–**3**.

determined between the OD1 of S (side chain)-ASP307 (with 3.14 Å bond distance)/O of M (main chain)-SER157(with 2.93 Å bond distance)/O of M (main chain)-PRO312 (with 2.88 Å bond distance) and nitrogen atom of dipya ligand. Unlike, major H-interaction for the complex **1** calculated at −3.5 kcal/mol energy value is defined between the NE2 of S (side chain)-HIS280 (with 3.05 and 2.80 Å bond distance) and oxygen atom belonging to acetate ligand. In brief, the docking and in vitro results are a remarkable scientific report for mixed-ligand (6-mpa and dipya) metal complexes.

4. Conclusion

The complexes **1**–**3** {[Cu(6-mpa)(dipya)(OAc)]·3H_2O, (**1**), [Co(6-mpa)(dipya)Cl_2]·2H_2O, (**2**), [Zn(6-mpa)$_2$(dipya)], (**3**)} were firstly synthesized and their structure characterizations were performed by XRD, LC-MS/MS, NMR, FT−IR and UV−Vis spectra. The IC_{50} values of the synthesized complexes **1**–**3** for α-glucosidase inhibition were found range from 513.10 to >600 μM range. According to these results, complex **1** has the most effective inhibitory activity against α-glucosidase. Furthermore, TD/DFT calculations with HSEh1PBE method and 6-311G(d,p)/LanL2DZ basis set were fulfilled to investigate the detailed structural, vibrational and electronic properties. Electronic spectra and theoretical results for the complexes **1**–**3** demonstrate metal−ligand and ligand−ligand charge transfer assigned as $n\rightarrow\pi^*$ and $\pi\rightarrow\pi^*$ transitions. It is clearly determined that NBO results confirm the coordination between LP electrons of the donor N/O/Cl atoms and M(II) ions in complexes **1**–**3**. It is concluded that there is a well agreement between the theoretical and corresponding experimental results. According to the NLO results, it could be estimated that the complex **2** is a powerful indicator for microscopic second−order NLO property while the complexes **1** and **3** are remarkable indicator for third−order NLO property. Considering in vitro and docking studies, present paper is a scientific study of mixed-ligand metal complexes containing 6-mpa and dipya ligands. Finally, it is foreseen that the better values in the NLO and IC_{50} parameters of new complexes to be synthesized may be possible with the change of substitute and metals in coordination.

Acknowledgements

This work was supported by the Scientific and Technological Research Council of Turkey (TÜBİTAK) (Project Number: MFAG−117F235).

Appendix A. Supplementary data

Supplementary data to this article can be found online at https://doi.org/10.1016/j.molstruc.2019.07.039.

References

[1] K.D. Demadis, S.D. Katarachia, Metal−phosphonate chemistry: synthesis, crystal structure of calcium−amino tris− (methylene phosphonate) and inhibition of CaCO3 crystal growth, Phosphorus, Sulfur, and Silicon 179 (2004) 627−648.
[2] J.G. Mao, Structures and luminescent properties of lanthanide phosphonates, Coord. Chem. Rev. 251 (2007) 1493−1520.
[3] J. Monot, M. Petit, S.M. Lane, I. Guisle, J. Léger, C. Tellier, D.R. Talham, B. Bujoli, Towards zirconium phosphonate−based microarrays for probing DNA− protein interactions: critical influence of the location of the probe anchoring groups, J. Am. Chem. Soc. 130 (2008) 6243−6251.
[4] A.M. Hardy, R.L. LaDuca, Synthesis and structure of a cobalt dicyanamide chain coordination polymer incorporating a long−spanning hydrogen−bonding capable diimine with a novel binodal (4,6)−connected supramolecular topology, Inorg. Chem. Commun. 12 (2009) 308−311.
[5] J. Umeda, M. Suzuki, M. Kato, M. Moriya, W. Sakamoto, T. Yogo, Proton conductive inorganic−organic hybrid membranes functionalized with phosphonic acid for polymer electrolyte fuel cell, J. Power Sources 195 (2010) 5882−5888.
[6] B.Y. Saito, J. Takemoto, B. Hutchinson, K. Nakamoto, Infrared studies of coordination compounds containing low-oxidation- state metals. I. Tris(2,2'-bipyridine) and tris(1,l0-phenanthroline) complexes, Inorg. Chem. 11 (1972) 2003−2011.
[7] V. Amani, N. Safari, H.R. Khavasi, Synthesis, characterization and crystal structure determination of iron(III) hetero-ligand complexes containing 2,20-bipyridine, 5,50-dimethyl-2,20-bipyridine and chloride, [Fe(bipy)Cl_4][bipy·H] and [Fe(dmbipy)$_2Cl_2$][$FeCl_4$], Polyhedron 26 (2007) 4257−4262.
[8] S.M. Mobin, A.K. Saini, V. Mishra, A. Chaudhary, A series of new heteroleptic Hg(II) complexes: synthesis, crystal structures and photophysical properties, Polyhedron 110 (2016) 131−141.
[9] C.Y. Cai, L. Rao, Y. Rao, J.X. Guo, Z.Z. Xiao, J.Y. Cao, Z.S. Huang, B. Wang, Analogues of xanthones−Chalcones and bis−chalcones as alpha−glucosidase inhibitors and anti−diabetes candidates, Eur. J. Med. Chem. 130 (2017) 51−59.
[10] J. Zhen, Y.J. Dai, T. Villani, D. Giurleo, J.E. Simon, Q.L. Wu, Synthesis of novel flavonoid alkaloids as alpha−glucosidase inhibitors, Bioorg, Med. Chem. 25 (2017) 5355−5364.
[11] U. Ghani, Re-exploring promising a-glucosidase inhibitors for potential development into oral anti-diabetic drugs: finding needle in the haystack, Eur. J. Med. Chem. 103 (2015) 133−162.
[12] S. Adisakwattana, P. Charoenlertkul, S. Yıbchok−Anun, α−Glucosidase inhibitory activity of cyanidin−3−galactoside and synergistic effect with acarbose, J. Enzym. Inhib. Med. Chem. 24 (2009) 65−69.
[13] J.L. Chiasson, R.G. Josse, R. Gomis, M. Hanefeld, A. Karasik, M. Laakso, STOP−NIDDM trial research group. Acarbose for the prevention of Type 2 diabetes, hypertension and cardiovascular disease in subjects with impaired glucose tolerance: facts and interpretations concerning the critical analysis of the STOPNIDDM Trial data, Lancet 359 (2002) 2072−2077.
[14] vd. Chiasson, C.M.M. Santos, M. Freitas, E. Fernandes, A comprehensive review on xanthone derivatives as α-glucosidase inhibitors, Eur. J. Med. Chem. 157 (2018) 1460−1479.
[15] M. Gollapalli, M. Taha, H. Ullah, M. Nawaz, L.M.R. AlMuqarrabun, F. Rahim, F. Qureshi, A. Mosaddik, N. Ahmat, K.M. Khan, Synthesis of Bis-indolylmethane sulfonohydrazides derivatives as potent α-Glucosidase

inhibitors, ides derivatives as potent α-Glucosidase inhibitors, Bioorg. Chem. 80 (2018) 112–120.
[16] H. Tang, F. Ma, D. Zhao, Z. Xue, Exploring the effect of salvianolic acid C on α-glucosidase: inhibition kinetics, interaction mechanism and molecular modelling methods, Process Biochem. 78 (2019) 178–188.
[17] C.M.M. Santos, M. Freitas, E. Fernandes, A comprehensive review on xanthone derivatives as α-glucosidase inhibitors, Eur. J. Med. Chem. 157 (2018) 1460–1479.
[18] M. Gollapalli, M. Taha, H. Ullah, M. Nawaz, L.M.R. AlMuqarrabun, F. Rahim, F. Qureshi, A. Mosaddik, N. Ahmat, K.M. Khan, Synthesis of Bis-indolylmethane sulfonohydrazides derivatives as potent α-Glucosidase inhibitors, Bioorg. Chem. 85 (2019) 33–48.
[19] E.C. Constable, P.J. Steel, N,N′-Chelating biheteroaromatic ligands; a survey, Coord. Chem. Rev. 93 (1989) 205–223.
[20] A. Usman, H.-K. Fun, S. Chantrapromma, M. Zhang, Z.-F. Chen, Y.-Z. Tang, S.-M. Shi, H. Liang, Diacetatobis(2-aminobenzothiazole)zinc(II), Acta Crystallogr. E59 (2003) m41–m43.
[21] H. Adams, N.A. Bailey, J.D. Crane, D.E. Fenton, J.M. Latour, J.M. Williams, Manganese (II) and iron (III) complexes of the tridentate ligands bis (benzimidazol−2−ylmethyl)−amine (L1) and−methylamine (L_2). Crystal structures of $[MnL_1\ (CH_3CO_2)_2]$,$[FeL_2Cl_3]$, and $[Fe_2L_{12}\ (\mu-O)\{\mu-(CH3)_3\ CO_2\}_2]$ $[ClO_4]_2$, J. Chem. Soc., Dalton Trans. 5 (1990) 1727–1735.
[22] W.L. Driessen, R.A.G. De Graaff, F.J. Parlevliet, J. Reedijk, R.M. De Vos, Transition metal compounds of the tridentate pyrazole substituted amine ligand bis (2− (3,5−dimethyl−1−pyrazolyl) ethyl) ethylamine (ddae). X−ray structures of $[Co(ddae)(NO_3)_2]$, $[Cu(ddae)(NO_3)(H_2O)](NO_3)$ and $[Cu(ddae)(Cl)_2]\cdot C_2H_5OH$, Inorg. Chim. Acta 216 (1994) 43–49.
[23] F. Grob, A. Müller-Hartmann, H. Vahrenkamp, Diphosphate−Zinc complexes with tridentate coligands, Eur. J. Inorg. Chem. 2000 (2000) 2363–2370.
[24] M. Gollapalli, M. Taha, M.T. Javid, N.B. Almandil, F. Rahim, A. Wadood, A. Mosaddik, M. Ibrahim, M.A. Alqahtani, Y.A. Bamarouf, Synthesis of benzothiazole derivatives as a potent α-glucosidase inhibitor, Bioorg. Chem. 85 (2019) 33–48.
[25] U. Ghani, Re-exploring promising a-glucosidase inhibitors for potential development into oral anti-diabetic drugs: finding needle in the haystack, Eur. J. Med. Chem. 103 (2015) 133–162.
[26] Y. Wang, L. Ma, Z. Li, Z. Du, Z. Liu, J. Qin, X. Wang, Z. Huang, L. Gu, A.S.C. Chen, Synergetic inhibition of metal ions and genistein on α-glucosidase, FEBS (Fed. Eur. Biochem. Soc.) Lett. 576 (2004) 46–50.
[27] Y. Shechter, S.J.D. Karlish, Insulin−like stimulation of glucose oxidation in rat adipocytes by vanadyl(IV) ions, Nature 284 (1980) 556–558.
[28] L. Coulston, P. Dandona, Insulin−like effect of zinc on adipocytes, Diabetes 29 (1980) 665–667.
[29] J.R.J. Sorenson, Copper complexes offer a physiological approach to treatment of chronic diseases, Prog. Med. Chem. 26 (1989), 437–568.
[30] R.A. Anderson, N. Cheng, N.A. Bryden, M.M. Polansky, N. Cheng, J. Chi, J. Feng, Elevated intakes of supplemental chromium improve glucose and insulin variables in individuals with type 2 diabetes, Diabetes 46 (1997) 1786–1791.
[31] H. Yasui, A. Tamura, T. Takino, H. Sakurai, Structure−dependent metallokinetics of antidiabetic vanadyl−picolinate complexes in rats: studies on solution structure, insulinomimetic activity, and metallokinetics, J. Inorg. Biochem. 91 (2002) 327–338.
[32] H. Yasui, A. Tamura, T. Takino, H. Sakurai, Structure−dependent metallokinetics of antidiabetic vanadyl−picolinate complexes in rats: studies on solution structure, insulinomimetic activity, and metallokinetics, J. Inorg. Biochem. 91 (2002) 327–338.
[33] N. Yasumatsu, Y. Yoshikawa, Y. Adachi, H. Sakurai, Antidiabetic copper(II)−picolinate: impact of the first transition metal in the metallopicolinate complexes, Bioorg. Med. Chem. 15 (2007) 4917–4922.
[34] Y. Yoshikawa, E. Ueda, K. Kawabe, H. Miyake, T. Takino, H. Sakurai, Y. Kojima, Development of new insulinomimetic zinc(II) picolinate complexes with a $Zn(N_2O_2)$ coordination mode: structure characterization, in vitro, and in vivo studies, J. Biol. Inorg. Chem. 7 (2002) 68–73 [Erratum: JBIC J. Biol. Inorg. Chem. 7 (2002) 560–561].
[35] Y. Yoshikawa, R. Hirata, H. Yasui, H. Sakurai, Alpha−glucosidase inhibitory effect of anti−diabetic metal ions and their complexes, Biochimie 91 (2009) 1339–1341.
[36] E. Ueda, Y. Yoshikawa, H. Sakurai, Y. Kojima, N.M. Kajiwara, In vitro α-glucosidase inhibitory effect of Zn(II) complex with 6-methyl-2-picolinmethylamide, Chem. Pharm. Bull. 53 (2005) 451–452.
[37] D. Avcı, S. Altürk, F. Sönmez, Ö. Tamer, A. Başoğlu, Y. Atalay, B.Z. Kurt, N. Dege, Three novel Cu(II), Cd(II) and Cr(III) complexes of 6-Methylpyridine-2-carboxylic acid with thiocyanate: synthesis, crystal structures, DFT calculations, molecular docking and α-Glucosidase inhibition studies, Tetrahedron 74 (2018) 7198–7208.
[38] D. Avcı, S. Altürk, F. Sönmez, Ö. Tamer, A. Başoğlu, Y. Atalay, B.Z. Kurt, N. Dege, A novel series of M(II) complexes of 6-methylpyridine-2-carboxylic acid with 4(5) methylimidazole: synthesis, crystal structures, α-glucosidase activity, density functional theory calculations and molecular docking, Appl. Organomet. Chem. 33 (2019) e4935.
[39] G.M. Sheldrick, SHELXT − integrated space-group and crystal-structure determination, Acta Crystallogr. A71 (2015) 3–8.
[40] C.F. Macrae, P.R. Edgington, P. McCabe, E. Pidcock, G.P. Shields, R. Taylor, M. Towler, J. van de Streek, Mercury visualization and analysis of crystal structures, J. Appl. Crystallogr. 39 (2006) 453–457.
[41] A.L. Spek, Structure validation in chemical crystallography, Acta Crystallogr. D65 (2009) 148–155.
[42] J. Rogan, D. Poleti, L. Karanović, G. Bogdanović, A. Spasojević-de Biré, D.M. Petrović, Mixed ligand Co(II), Ni(II) and Cu(II) complexes containing terephthalato ligands. Crystal structures of diaqua(2,2'-dipyridylamine)(terephthalato)metal(II) trihydrates (metal = cobalt or nickel), Polyhedron 19 (2000) 1415–1421.
[43] D. Bose, Sk H. Rahaman, G. Mostafa, R.D.B. Walsh, M.J. Zaworotko, B.K. Ghosh, Synthesis, structure and properties of $[Zn(dpa)(N_3)_2]$ and $[Zn(dpa)(N_3)(NO_3)]_2$ (dpa=2,2'-dipyridylamine): composition tailored architectures, Polyhedron 23 (2004) 545–552.
[44] H. Sun, W.N. Ding, X.T. Song, D. Wang, M.Z. Chen, K.L. Wang, Y.Z. Zhang, P. Yuan, Y. Ma, R.L. Wang, R.H. Dodd, Y.M. Zhang, K. Lu, P. Yu, Bioorg. Med, Chem. Lett. 27 (2017) 3226–3230.
[45] M.J. Frisch, G.W. Trucks, H.B. Schlegel, G.E. Scuseria, M.A. Robb, J.R. Cheeseman, G. Scalmani, V. Barone, B. Mennucci, G.A. Petersson, H. Nakatsuji, M. Caricato, X. Li, H.P. Hratchian, A.F. Izmaylov, J. Bloino, G. Zheng, J.L. Sonnenberg, M. Hada, M. Ehara, K. Toyota, R. Fukuda, J. Hasegawa, M. Ishida, T. Nakajima, Y. Honda, O. Kitao, H. Nakai, T. Vreven, J.A. Montgomery Jr., J.E. Peralta, F. Ogliaro, M. Bearpark, J.J. Heyd, E. Brothers, K.N. Kudin, V.N. Staroverov, R. Kobayashi, J. Normand, K. Raghavachari, A. Rendell, J.C. Burant, S.S. Iyengar, J. Tomasi, M. Cossi, N. Rega, J.M. Millam, M. Klene, J.E. Knox, J.B. Cross, V. Bakken, C. Adamo, J. Jaramillo, R. Gomperts, R.E. Stratmann, O. Yazyev, A.J. Austin, R. Cammi, C. Pomelli, J.W. Ochterski, R.L. Martin, K. Morokuma, V.G. Zakrzewski, G.A. Voth, P. Salvador, J.J. Dannenberg, S. Dapprich, A.D. Daniels, O. Farkas, J.B. Foresman, J.V. Ortiz, J. Cioslowski, D.J. Fox, Gaussian 09, Revision D.01, Gaussian, Inc., Wallingford, CT, 2013.
[46] R. Dennington, T. Keith, J. Millam, GaussView, Semichem Inc., Shawnee Mission KS, 2009, Version 5.
[47] J. Heyd, G.E. Scuseria, Efficient hybrid density functional calculations in solids: assessment of the Heyd-Scuseria-Ernzerhof screened Coulomb hybrid functional, J. Chem. Phys. 121 (2004) 1187–1192.
[48] A.V. Krukau, O.A. Vydrov, A.F. Izmaylov, G.E. Scuseria, Influence of the exchange screening parameter on the performance of screened hybrid functionals, J. Chem. Phys. 125 (2006) 224106.
[49] M.J. Frisch, J.A. Pople, J.S. Binkley, Self-consistent molecular orbital methods 25. Supplementary functions for Gaussian basis set, J. Chem. Phys. 80 (1984) 3265–3269.
[50] P.J. Hay, W.R. Wadt, Ab initio effective core potentials for molecular calculations. Potentials for the transition metal atoms Sc to Hg, J. Chem. Phys. 82 (1985) 270–283.
[51] E. Runge, E.K.U. Gross, Density-functional theory for time-dependent systems, Phys. Rev. Lett. 52 (1984) 997–1000.
[52] S. Miertus, E. Scrocco, J. Tomasi, Electrostatic interaction of a solute with a continuum. A direct utilizaion of Ab initiomolecular potentials for the prevision of solvent effects, J. Chem. Phys. 55 (1981) 117–129.
[53] E.D. Glendening, A.E. Reed, J.E. Carpenter, F. Weinhold, NBO Version3.1, TCI, University of Wisconsin, Madison, 1998.
[54] J.-M. Yang, C.-C. Chen, GEMDOCK: a generic evolutionary method for molecular docking, Proteins 55 (2004) 288–304.
[55] B.-M. Kukovec, Z. Popović, B. Kozlevčar, Z. Jagličić, 3D supramolecular architectures of copper(II) complexes with 6-methylpicolinic and 6-bromopicolinic acid: synthesis, spectroscopic, thermal and magnetic properties, Polyhedron 27 (2008) 3631–3638.
[56] S. Altürk, D. Avcı, A. Başoğlu, Ö. Tamer, Y. Atalay, N. Dege, Copper(II) complex with 6-methylpyridine-2-carboxyclic acid: experimental and computational study on the XRD, FT-IR and UV−Vis spectra, refractive index, band gap and NLO parameters, Spectrochim. Acta 190 (2018) 220–230.
[57] S. Altürk, D. Avcı, Ö. Tamer, Y. Atalay, O. Şahin, A cobalt(II) complex with 6-methylpicolinate: synthesis, characterization, second- and third-order nonlinear optical properties, and DFT calculations, J. Phys. Chem. Solids 98 (2016) 71–80.
[58] B.-M. Kukovec, P.D. Vaz, Z. Popović, M.J. Calhorda, K. Furić, G. Pavlović, M.R. Linarić, Pseudopolymorphismin nickel(II) complexeswith 6-methylpicolinic acid. Synthesis, structural, spectroscopic, thermal and DFT study, Cryst. Growth Des. 8 (2008) 3465–3473.
[59] Zouaoui Setifi, Fatima Setifi, Mohamed Ghazzali, Malika El-Ghozzi, Daniel Avignant, Olivier Pérez, Jan Reedijk, Adipate as a tetradentate bridging ligand: synthesis, structure and properties of Cu(II) and Ni(II) compounds with 2,2′-dipyridylamine as a terminal co-ligand, Polyhedron 75 (2014) 68–72.
[60] A.P. Scott, L. Radom, Harmonic vibrational frequencies: an evaluation of Hartree-Fock, Møller-Plesset, quadratic configuration interaction, density functional theory, and Semiempirical scale factors, J. Phys. Chem. 100 (1996) 16502–16513.
[61] G. Varsanyi, Assignments for Vibrational Spectra of Seven Hundred Benzene Derivatives, Academic Kiaclo, Budapest, 1973.
[62] T. hui Hu, X. Zhang, Q. Wang, W. sheng You, C. ying Huang, Y. Fang, Two metal complexes supported by $\{VO3\}_n^{n-}$ chains: hydrothermal syntheses and crystal structures of $[M(dpa)V_2O_6]$ (M = Zn(II) and Cu(II); dpa = 2,2'-dipyridylamine), J. Chem. Crystallogr. 41 (2011) 64–68.
[63] D. Avcı, S. Altürk, F. Sönmez, Ö. Tamer, A. Başoğlu, Y. Atalay, B.Z. Kurt, D. Öztürk, N. Dege, A new dinuclear copper (II) complex of 2,5−Furandicarboxyclic acid with 4(5)−Methylimidazole as a high potential

α–glucosidase inhibitor: synthesis, Crystal structure, Cytotoxicity study, and TD/DFT calculations, Appl. Organomet. Chem. 33 (2019), e4725.
[64] J. Pons, R. March, J. Rius, J. Ros, Zinc complexes of 6-methyl-2-pyridinecarboxylic acid. Crystal structure of $[Zn(MeC_5H_3NCOO)_2(H_2O)]\cdot H_2O$, Inorg. Chim. Acta 357 (2004) 3789–3792.
[65] S.I. Gorelsky, SWizard ProgramRevision 4.5,, University of Ottawa, Ottawa, Canada, 2010. http://www.sg.chem.net/.
[66] İ. Şişman, A. Başoğlu, Effect of Se content on the structural, morphological and optical properties of $Bi_2Te_{3-y}Se_y$ thin films electrodeposited by under potential deposition technique, Mater. Sci. Semicond. Process. 54 (2016) 57–64.
[67] W. Yang, R.G. Parr, Hardness, softness, and the fukui function in the electronic theory of metals and catalysis, Proc. Natl. Acad. Sci. U.S.A. 82 (1985) 6723–6726.
[68] A.E. Reed, F. Weinhold, Natural bond orbital analysis of near-Hartree–Fock water dimer, J. Chem. Phys. 78 (1983) 4066–4073.
[69] J.P. Foster, F. Weinhold, Natural hybrid orbitals, J. Am. Chem. Soc. 102 (1980) 7211–7218.
[70] J. Sponer, P. Hobza, DNA base amino groups and their role in molecular interactions: ab initio and preliminary density functional theory calculations, Int. J. Quantum Chem. 57 (1996) 959–970.
[71] S.R. Gadre, I.H. Shrivastava, Shapes and sizes of molecular anions via topographical analysis of electrostatic potential, J. Chem. Phys. 94 (1991) 4384–4390.
[72] D.S. Chemla, J. Zysss, Nonlinear Optical Properties of Organic Molecules and Crystals, Academic Press, Orlando, FL, 1987.
[73] K. Kamada, M. Ueda, H. Nagao, K. Tawa, T. Sugino, Y. Shmizu, K. Ohta, Molecular design for organic nonlinear optics: polarizability and hyperpolarizabilities of furan homologues investigated by ab initio molecular orbital method, J. Phys. Chem. A 104 (2000) 4723–4734.
[74] B.M. Pierce, A theoretical analysis of third-order nonlinear optical properties of linear polyenes and benzene, J. Chem. Phys. 91 (1989) 791–811.
[75] L.-T. Cheng, W. Tam, S.H. Stevenson, G.R. Meredith, G. Rikken, S.R. Marder, Experimental investigations of organic molecular nonlinear optical polarizabilities. 1. Methods and results on benzene and stilbene derivatives, J. Phys. Chem. 95 (1991) 10631–10643.
[76] P. Kaatz, E.A. Donley, D.P. Shelton, A comparison of molecular hyperpolarizabilities from gas and liquid phase measurements, J. Chem. Phys. 108 (1998) 849–856.
[77] M. Stahelin, D.M. Burland, J.E. Rice, Solvent dependence of the second order hyperpolarizability in p-nitroaniline, Chem. Phys. Lett. 191 (1992) 245–250.
[78] C. Adant, M. Dupuis, J.L. Bredas, Ab initio study of the nonlinear optical properties of urea: electron correlation and dispersion effects, Int. J. Quantum Chem. 56 (2004) 497–507.
[79] M. Taha, N. Hadiani Ismail, S. Lalani, M. Qaiser Fatmi, Atia-tul-Wahab, S. Siddiqui, K.M. Khan, S. Imran, M. Iqbal Choudhary, Synthesis of novel inhibitors of α-glucosidase based on the benzothiazole skeleton containing benzohydrazide moiety and their molecular docking studies, Eur. J. Med. Chem. 92 (2015) 387–400.
[80] M. Taha, N. Hadiani Ismail, M. Syukri Baharudin, S. Lalani, S. Mehboob, K.M. Khan, S. Yousuf, S. Siddiqui, F. Rahim, M.I. Choudhary, Synthesis crystal structure of 2-methoxybenzoylhydrazones and evaluation of their α-glucosidase and urease inhibition potential, Med. Chem. Res. 24 (2015) 1310–1324.
[81] J.-W. Zheng, L. Ma, Silver(I) complexes of 2,4-dihydroxybenzaldehyde–amino acid Schiff bases-Novel noncompetitive α-glucosidase inhibitors, Bioorg. Med. Chem. Lett 25 (2015) 2156–2216.
[82] J.-W. Zheng, L. Ma, Metal complexes of anthranilic acid derivatives: a new class of non-competitive α-glucosidase inhibitors, Chin. Chem. Lett. 27 (2016) 627–630.

Update

Journal of Molecular Structure

Volume 1246, Issue , 15 December 2021, Page

DOI: https://doi.org/10.1016/j.molstruc.2021.131223

Journal of Molecular Structure 1246 (2021) 131223

Contents lists available at ScienceDirect

Journal of Molecular Structure

journal homepage: www.elsevier.com/locate/molstr

Corrigendum

Corrigendum to 'Novel Cu(II), Co(II) and Zn(II) metal complexes with mixed-ligand: Synthesis, crystal structure, α-glucosidase inhibition, DFT calculations, and molecular docking' [Journal of Molecular Structure 1197 (2019) 645-655]

Davut Avcı[a,*], Sümeyye Altürk[a], Fatih Sönmez[b], Ömer Tamer[a], Adil Başoğlu[a], Yusuf Atalay[a], Belma Zengin Kurt[c], Necmi Dege[d]

[a] Sakarya University, Faculty of Arts and Sciences, Department of Physics, 54187, Sakarya, Turkey
[b] Sakarya University of Applied Sciences, Pamukova Vocational School, 54055, Sakarya, Turkey
[c] Bezmialem Vakif University, Faculty of Pharmacy, Department of Pharmaceutical Chemistry, 34093, Istanbul, Turkey
[d] Ondokuz Mayıs University, Faculty of Arts and Sciences, Department of Physics, 55139, Samsun, Turkey

DOI of original article: https://doi.org/10.1016/j.molstruc.2019.07.039
The authors regret that the project number was incorrectly given in the article.
The authors would like to apologise for any inconvenience caused.
The corrected part is given as follows:

Acknowledgements

This work was supported by the Scientific and Technological Research Council of Turkey (TÜBİTAK) (Project Number: MFAG-117F234).

DOI of original article: 10.1016/j.molstruc.2019.07.039
* Corresponding author.
E-mail address: davci@sakarya.edu.tr (D. Avcı).

https://doi.org/10.1016/j.molstruc.2021.131223